16th World Conference on Earthquake, 16WCEE 2017

Santiago Chile, January 9th to 13th 2017

Paper N° 4527

Registration Code: S-I1463146654

Stochastic dynamic response analysis of bridge piers in deep water under combined earthquake and wave actions

Y. Ding[(1)], S.B. Meng[(2)], Y.D. Shi[(3)]

[(1)] Professor, Key Laboratory of Coast Civil Structure Safety of Ministry of Education, Tianjin University, Tianjin, China. dingyang@tju.edu.cn
[(2)] Ph.D Candidate, Key Laboratory of Coast Civil Structure Safety of Ministry of Education, Tianjin University, Tianjin, China. sunshinekahn@126.com
[(3)] Assistant professor, Key Laboratory of Coast Civil Structure Safety of Ministry of Education, Tianjin University, Tianjin, China. yundong@tju.edu.cn

Abstract

Earthquake and wave actions may be simultaneously applied to bridge piers in deep water. It is necessary to calculate the dynamic response of bridge piers under combined earthquake and wave actions. In order to consider the randomness of earthquake and wave action, stochastic dynamic response analysis is adopted. The interaction between bridge piers and water can be considered into two parts: the hydrodynamic pressure and wave action. Since most bridge piers belong to large-scale cylinder, the hydrodynamic pressure is established using radiation wave theory, and the wave action is considered by the diffraction theory. Based on the pseudo excitation method, a stochastic dynamic analysis method for bridge piers in deep water under combined actions of earthquake and wave is developed. A circle solid pier is calculated with a sectional diameter of 5 m and a height of 24.7 m. The Clough-Penzien spectrum is used as the earthquake acceleration spectrum and the Bretschneider-Mitsuyasu spectrum is used as the wave height spectrum. Stochastic dynamic responses of bridge piers under the earthquake action, wave action and combined actions of earthquake and wave, are analyzed respectively. Different relative water depths and earthquake acceleration amplitudes are considered for the analysis of the numerical model under earthquake action. While the model under wave action is caculated, different wave heights and relative water depths are analyzed and compared. Moreover, in order to compare with the response under combined earthquake and wave actions, the response under the direct superpositon of two individual actions should be achieved. The results show that the stochanic dynamic response of the pier in deep water is increasing because of the influence of the hydrodynamic pressure. For a pier with a fixed water depth under different earthquake acceleration amplitudes, the increased percentage of the internal force power spectrums at the bottom of piers is identical, considering the effect of the hydrodynamic pressure. With relative water depth becoming deeper, the effect of the hydrodynamic pressure to the internal force power spectrums at the bottom of the pier becomes more significant. Because the attached mass generated by the pier's elastic motion in the water has little effect on the frequency response function of the pier, stochanic dynamic responses under combined earthquake and wave actions are identical with these under the direct superposition of two individual actions.

Keywords: *bridge piers in deep water, earthquake action, wave action, pseudo excitation method*

1. Introduction

With the development of economy, the number of bridges, especially sea-crossing and river-crossing bridges, increases faster. There are already a large number of studies about the dynamic responses of multiform bridges under earthquakes [1, 2]. As the sea-crossing or river-crossing bridges are in a water environment, it needs to consider the interaction between piers and water under earthquakes. Generally, the interaction can be considered into two parts: the hydrodynamic pressure generated by moving piers in static water and the wave action generated by static piers in moving water. Earthquake ground motion and wave height are both random processes, therefore it is necessary to analyze the response of bridge piers under combined earthquake and wave actions using the stochastic vibration method.

The studies on analysis method of the interaction between piers and water mainly include numerical method and semi-numerical method. Ozdemir Z [3] proposed a fully nonlinear liquid-solid coupling finite elements approach based on the numerical method. Yeung RW [4] studied on the hydrodynamic attached mass and damping of a vertical column in finitely deep water. Keming S [5] deduced the hydrodynamic pressure formula of an axisymmetric structure based on the Trefftz-complete function. Lai W [6] deduced the exterior attached hydrodynamic pressure of circle piers based on the linear radiation wave theory. There are two methods normally adopted for calculation of the wave force, including the diffraction wave theory for large-diameter columns and Morison function for small-diameter columns [7-9]. The studies shown above mainly analyzed the effects of the interaction of piers and water for piers or bridges in time domain, and the effect is related to the earthquake wave [10]. To date, there are only limited number of studies on stochastic dynamic responses analysis of bridge piers in deep water under the earthquake action or combined earthquake and wave actions.

Stochastic vibration methods applied on engineering structures mainly include the pseudo excitation method and Monte Carlo method. Lu F [11] proposed an efficient algorithm for non-stationary random vibration of vehicle-bridge systems basing on the pseudo excitation method. Fan LC [12] investigated the response characteristics of long-span cable-stayed bridges under seismic action with spatial variation by using the pseudo excitation method. Considering the uncertainties in the ground motion characteristics through the Monte Carlo method, Moghaddasi M [13] evaluated the influence of foundation flexibility on the structural seismic response. However, these studies only analyzed the responses under an single load. In this paper, based on the pseudo excitation method, this paper establishes a stochastic dynamic responses analysis method for bridge piers in deep water under combined earthquake and wave actions in linear scope. Stochastic dynamic responses of bridge piers under the earthquake action, the wave action and combined earthquake and wave actions are analyzed respectively.

2. Stochastic dynamic analysis method of bridge piers in deep water under combined earthquake and wave actions

2.1 Hydrodynamic pressure based on radiation wave theory

Generally, the radiation wave theory uses the separation variable method or Green function to obtain general solutions of the velocity potential of the Laplace equation, and solve the constant of the velocity potential by water's boundary condition. After that, the expression of the hydrodynamic pressure from the Bernoulli equation can be obtained, and the deduced process is privided in reference [5] in detail.

The structure-fluid-ground system is illustrated in Fig.1. The water is assumed to be irrotational, inviscid, and incompressible; and the motion of the water is limited to small amplitudes during the earthquake action.

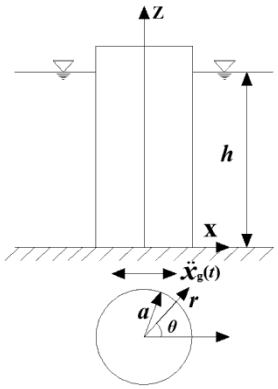

Fig. 1 –Structure-fluid-ground system

In the cylinder coordinate, when the ground undergoes a harmonic motion with frequency ω, the velocity potential of the water can be expressed by the complex form $\Phi(r,\theta,z,t)=\phi(r,\theta,z)e^{i\omega t}$ according to the radiation wave theory. Substitute $\phi(r,\theta,z)$ into the Laplace equation, the flow control equation is

$$\frac{\partial^2\phi}{\partial r^2}+\frac{1}{r}\frac{\partial\phi}{\partial r}+\frac{1}{r^2}\frac{\partial^2\phi}{\partial\theta^2}+\frac{\partial^2\phi}{\partial z^2}=0 \tag{1}$$

$\phi(r,\theta,z)$ can be expressed by introducing the Trefftz-complete function and meets boundary conditions as shown below

$$\frac{\partial\phi}{\partial z}-\frac{\omega^2}{g}\phi=0, z=h \tag{2}$$

$$\frac{\partial\phi}{\partial z}=0, z=0 \tag{3}$$

$$\frac{\partial\phi}{\partial r}=\frac{\partial U}{\partial t}\cos\theta, z=a, 0\le z\le h \tag{4}$$

$$\lim_{r\to\infty}\sqrt{r}\left(\frac{\partial\phi}{\partial r}-ik\phi\right)=0 \tag{5}$$

Eqs. (2)-(5) are the free surface bounary condition, the bottom bounary condition, the interface surface bounary condition and Sommerfeld radition bounary condition, respectively; $i=\sqrt{-1}$; a is the pier's radius; h is water depth; $k=\omega/c$, where c denotes the sound velocity in the water; and U is the absolute displacement of the pier, including the rigid displacement and elastic displacement. The full velocity potential can be taken into two parts: the velocity potential Φ_1 generated by the pier's rigid motion and velocity potential Φ_2 generated by the pier's elastic motion. They can be derived by Eqs. (1)-(5). Note that the effect of free surface wave is ignored in the analysis.

According to the the small amplitudes wave theory, the hydrodynamic pressure F of the pier's surface along a unit height is

$$F=\rho\int_0^{2\pi}\frac{\partial\Phi(r,\theta,z,t)}{\partial t}a\cos\theta\,\mathrm{d}\theta \tag{6}$$

where ρ is the water density. Substitute the rigid velocity potential Φ_1 and elastic velocity potential Φ_2 into Eq. (6), the hydrodynamic pressure can be expressed as

$$F_1(r,a,t)\big|_{r=a} = \rho\int_0^{2\pi}\frac{\partial\Phi_1}{\partial t}a\cos\theta\,\mathrm{d}\theta = -M_1\left[\ddot{x}_g\right] \tag{7}$$

$$F_2(r,a,t)\big|_{r=a} = \rho\int_0^{2\pi}\frac{\partial\Phi_2}{\partial t}a\cos\theta\,\mathrm{d}\theta = -M_2\left[\ddot{x}\right] \tag{8}$$

where F_1 and F_2 is the hydrodynamic pressure generated by the ground motion and the elastic vibration of the structure respectively; $\ddot{x}_g$ and $\ddot{x}$ are the harmonic ground motion acceleration and elastic vibration acceleration of the structure respectively. M_1 and M_2 are the rigid attached mass matrix and elastic attached mass matrix respectively. M_1 is a diagonal matrix, and the ith diagonal element is

$$m_{1_i} = -2\pi a\rho\int_{\Gamma_i}\sum_{m=1}^{M}\sin\left(\lambda_m^{'}h\right)\bar{K}_1\left(\beta_m a\right)\frac{\cos\left(\lambda_m^{'}z\right)}{\lambda_m^{'}\beta_m h}\mathrm{d}z \tag{9}$$

The elements in the mass matrix M_2 are

$$m_{2_{ij}} = -2\pi a\rho\int_{\Gamma_i}\sum_{m=1}^{M}\cos\left(\lambda_m^{'}z_j\right)L_j\bar{K}_1\left(\beta_m a\right)\frac{\cos\left(\lambda_m^{'}z\right)}{\beta_m h}\mathrm{d}z \tag{10}$$

in which

$$\bar{K}_1\left(\beta_m a\right)=\frac{K_1\left(\beta_m a\right)}{K_1^{'}\left(\beta_m a\right)},\quad K_1^{'}\left(\beta_m a\right)=\left.\frac{\partial K_1\left(\beta_m r\right)}{\partial\beta_m r}\right|_{r=a} \tag{11}$$

$$\lambda_m^{'} = \beta_m = \frac{\left(2m-1\right)\pi}{2h} \tag{12}$$

where Γ_i denotes the integral interval of the ith node; L_i is the ith element's length; Z_i is the ith node's coordinate of axis Z; and $K_1(\beta_m r)$ is the modified Bessel function of the second kind and first order.

2.2 Wave force based on diffraction theory

Generally, the velocity potential of the diffraction problem can be considered into two parts: the incident potential ϕ_i and diffraction potential ϕ_d. Substitute both potentials into the Bernoulli equation, the wave force acting on a circle pier can be solved [10]. In the cylinder coordinate, the incident potential $\phi_i(r,\theta,z)$ should be expressed as

$$\phi_i\left(r,\theta,z\right)=-\frac{igA}{\omega}\frac{\cosh kz}{\cosh kh}\sum_{m=0}^{\infty}\varepsilon_m i^m J_m\left(kr\right)\cos m\theta \tag{13}$$

where $i=\sqrt{-1}$; $\varepsilon_m=\begin{cases}1 & (m=0)\\ 2 & (m\geq 1)\end{cases}$; A is the wave amplitude; $J_m(kr)$ is the Bessel function of the first kind; and k is the wave number.

The diffraction potential $\phi_d(r,\theta,z)$ can be expressed as

$$\phi_d\left(r,\theta,z\right)=-\frac{igA}{\omega}\frac{\cosh kz}{\cosh kh}\sum_{m=0}^{\infty}\varepsilon_m i^m A_m H_m\left(kr\right)\cos m\theta \tag{14}$$

where $H_m(kr)$ denotes the Hankel function of the first kind. The incident potential and diffraction potential should meet the boundary conditions below

$$\frac{\partial \phi_d}{\partial z} - \frac{\omega^2}{g}\phi_d = 0, z = 0 \tag{15}$$

$$\frac{\partial \phi_d}{\partial z} = 0, z = -h \tag{16}$$

$$\frac{\partial \phi_d}{\partial r} + \frac{\partial \varphi_i}{\partial r} = 0, z = a \tag{17}$$

$$\lim_{r\to\infty} \sqrt{r}\left(\frac{\partial \phi_d}{\partial r} - ik\phi_d\right) = 0 \tag{18}$$

Substitute the incident potential and diffraction potential into the boundary conditions and the full velocity potential space factor of the whole wave field can be solved as

$$\phi(r,\theta,z) = -\frac{igA}{\omega}\frac{\cosh kz}{\cosh kh}\sum_{m=0}^{\infty}\varepsilon_m i^m\left[J_m(kr) - \frac{J_m^{'}(ka)}{H_m^{'}(ka)}H_m(kr)\right]\cos m\theta \tag{19}$$

Using the orthogonality of the cosine function and Wornkcy identical equation, the wave force acting on the pier structure can be expressed in Eq. (20) by substituting Eq. (19) into the Bernoulli equation.

$$P(z) = -\frac{4A\rho g}{kH_1^{(1)'}(ka)}\frac{\cosh kz}{\cosh kh}e^{ikx_0 - i\omega x_0} \tag{20}$$

where x_0 is the space position with the incident wave spreading direction on the pier's central axis; and $H_1^{(1)'}(k_0a)$ is the Hankel function of the first kind and first order. The Wornkcy identical equation is

$$J_m(z)H_m^{'}(z) - J_m^{'}(z)H_m(z) = \frac{2}{\pi z} \tag{21}$$

Considering the phase difference of incident wave motion in different horizontal location at the same time, the wave force acting on the circle pier is the real part of $P(z)$ in Eq. (20).

2.3 Establishment of stochastic dynamic analysis method

Substitute the hydrodynamic pressure obtained using the radiation wave theory and the wave force obtained using the diffraction theory into the dynamic equation of the pier, it gives

$$(M + M_2)\ddot{x} + C\dot{x} + Kx = -(M + M_1)I\ddot{x}_g(t) + P(t) \tag{22}$$

where M, C and K are the mass, damping and stiffness matrices of the pier; and $P(t)$ is the wave force. Only the wave action is considered when $P(t)$ is zero, and only the earthquake action is considered when M_1 and M_2 are zero.There is no correlation between earthquake ground motions and wave heights, thus the correlation coefficient is zero. Assuming that $Z(t) = -(M + M_1)I\ddot{x}_g(t) + P(t)$, the auto-correlation function $R_{ZZ}(\tau)$ of it which is used for the Fourier transform is

$$R_{ZZ}(\tau) = (M + M_1)IR_{\ddot{x}_g\ddot{x}_g}(\tau)I^T(M + M_1) + R_{PP}(\tau) \tag{23}$$

where $R_{\ddot{x}_g\ddot{x}_g}(\tau)$ and $R_{PP}(\tau)$ are the auto-correlation functions of $\ddot{x}_g$ and $P(t)$ respectively. The power spectrum $S_{ZZ}(\omega)$ of $Z(t)$ is

$$S_{ZZ}(\omega) = (M + M_1)IS_{\ddot{x}_g\ddot{x}_g}(\omega)I^T(M + M_1) + S_{PP}(\omega) \tag{24}$$

where $S_{\ddot{X}_g\ddot{X}_g}(\omega)$ is the earthquake acceleration spectrum; and the wave force spectrum $S_{pp}(\omega)$ can be written as

$$S_{PP}(\omega)=\left(\frac{4A\rho g}{k_0 H_1^{(1)'}(k_0 a)}\frac{\cosh kz}{\cosh kh}\right)^2 S_{HH}(\omega) \tag{25}$$

where $S_{HH}(\omega)$ is the wave height spectrum.

Generally, $S_{ZZ}(\omega)$ is a positive definite or positive semi-definite symmetric matrix. Assuming that the matrix's rank is r_0, it can be decomposited into the product of the $n\times r_0$ matrix L and its transposition matrix L^{T} accroding to the $\mathrm{LDL}^{\mathrm{T}}$ decomposition as

$$S_{ZZ}(\omega)=LL^{\mathrm{T}} \tag{26}$$

By means of the method established by Lin JH [14], a pesudo excitation is created as

$$p=Le^{i\omega t} \tag{27}$$

Substitute the pesudo excitation above into the dynamic equation, the pesudo displacement response $\tilde{x}$ is

$$\tilde{x}=H(\omega)Le^{i\omega t} \tag{28}$$

where the frequency response function $H(\omega)$ is

$$H(\omega)=1/\left[-\omega^2(M+M_2)+K+i\omega C\right] \tag{29}$$

The displacement response spectrum $S_{xx}(\omega)$, the internal force response spectrum $S_{FF}(\omega)$ and their square-variances σ_x and σ_F can be expressed respectively as

$$S_{xx}(\omega)=\tilde{x}\tilde{x}^{\mathrm{T}} \tag{30}$$

$$S_{FF}(\omega)=K\left(\tilde{x}\tilde{x}^{\mathrm{T}}\right)K^T \tag{31}$$

$$\sigma_x=\sqrt{\int_0^\infty S_{xx}(\omega)\mathrm{d}\omega} \tag{32}$$

$$\sigma_F=\sqrt{\int_0^\infty S_{FF}(\omega)\mathrm{d}\omega} \tag{33}$$

In order to apply stochastic dynamic results in engineering designs, the extreme value distributions, means and variances of responses can be calculated by random extreme value theory [15, 16].

3. Numerical example

3.1 Calculation model

A circle solid pier is calculated with a sectional diameter of 5 m and a height of 24.7 m. The calculated span, height, density and elastic modulus are 51.1 m, 4.25 m, 2500 kg/m^3 and 3.0×10^4 Mpa, respectively. The girder of 525000 kg is considered as a lumped mass acting on the top of the pier. In the numerical model, the pier is divided into 13 elements. The height is 0.7 m for the bottom element and 2 m for the others. The finite element model adopts smeared model to consider the reinforced concrete. The fundamental frequency of the model is 14.9 rad/s.

The Clough-Penzien spectrum is used as the earthquake acceleration spectrum $S_{\ddot{x}_g\ddot{x}_g}(\omega)$ and the Bretschneider-Mitsuyasu spectrum is used as the wave height spectrum $S_{HH}(\omega)$. The expressions are given as below.

$$S_{\ddot{x}_g\ddot{x}_g}(\omega)=\frac{\omega_g^4+4\zeta_g^2\omega_g^2\omega^2}{\left(\omega_g^2-\omega^2\right)^2+4\zeta_g^2\omega_g^2\omega^2}\frac{\omega^4}{\left(\omega_f^2-\omega^2\right)+4\zeta_f^2\omega_f^2\omega^2}S_0 \tag{34}$$

$$S_{HH}(\omega)=400.5\left(\frac{H_s}{T_{H_{1/3}}^2}\right)^2\frac{1}{\omega^5}\exp\left(-1605\left(\frac{1}{T_{H_{1/3}}\omega}\right)^4\right) \tag{35}$$

For both spectrums above, ω_g presents the predominant frequency and ζ_q is the damping ratio of the first order highpass filter respectively; ω_f and ζ_f are the parameters of the second order highpass filter; S_0 is the constant spectral density of the input white noise process; besides, H_s is the significant wave height; and $T_{H1/3}$ is the significant wave period. The frequency ranges, frequency spacings, durations and time intervals are [0, 20] rad/s, 0.05 rad/s, 4 s and 0.02 s, respectively. In order to analyze the responses results, two parameters are defined: the relative water depth $h_0=h/H$ where H is the pier's height; and the increased percentage $\Delta=(S_2-S_1)/S_1$ where S_1 is the power spectrum of internal forces with no water at a specific frequency ω; and S_2 is the power spectrum of internal forces with a relative water depth h_0 at the same frequency ω. In this paper, the nonlinear solitary wave generated by strong seismic attack is not considered.

3.2 Stochastic dynamic analysis of the pier in deep water under earthquake action

Stochastic dynamic analysis of the pier in deep water under earthquake action is calculated with six conditions. The relative water depth h_0 of 0.60 is chosen, and different earthquake acceleration amplitudes a_g of 0.1 g, 0.2 g and 0.4 g are adopted. Zero water depth is also considered for comparision. The shear force power spectrum and moment power spectrum of the pier's bottom at different conditions are shown in Figs.2 and 3 respectively. The figures show that the peak values of the shear force and moment power spectrums appear at the fundamental frequency of the pier. With the increase of earthquake acceleration amplitudes, the internal force power spectrums at the pier's bottom are increasing. Fig. 4 graphically shows the increased percentage Δ. As seen from the figure, the internal force power spectrums at the pier's bottom are affected by the hydrodynamic pressure with the same increased percentage Δ at different frequecies. The red circles in Fig.4 represent the increased percentage Δ at the peak value of the internal force power spectrums. Due to the hydrodynamic pressure, the peak value of the shear force power spectrum at the pier's bottom increases 13% ,while the peak value of the moment power spectrum at the pier's bottom increases only 4%.

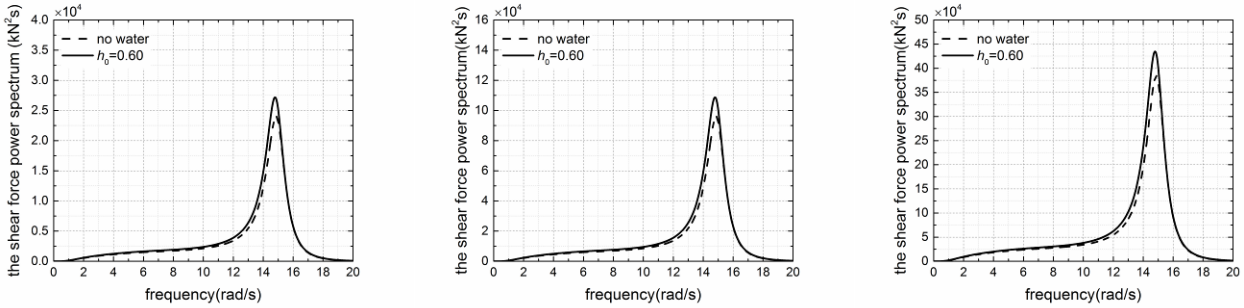

(a) a_g=0.1 g (b) a_g=0.2 g (c) a_g=0.4 g

Fig. 2 –The shear force power spectrum at the pier's bottom with no water and h_0=0.60

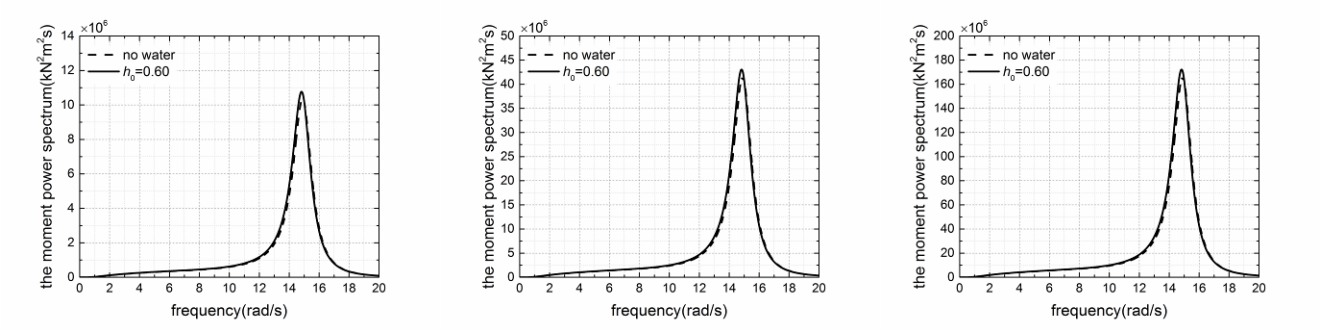

(a) a_g=0.1 g (b) a_g=0.2 g (c) a_g=0.4 g

Fig. 3 –The moment power spectrum at the pier's bottom with no water and h_0=0.60

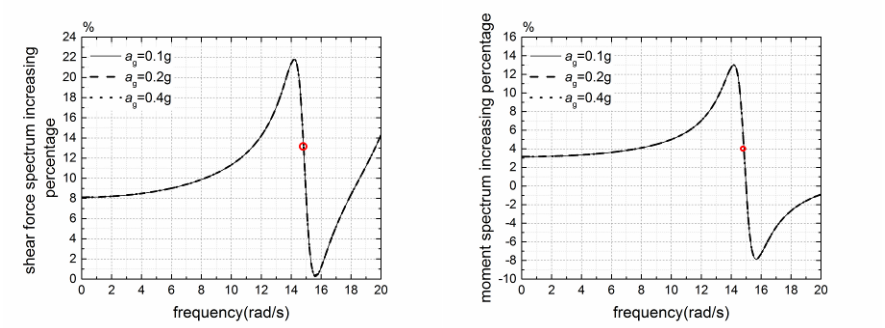

(a) The shear force power spectrum (b) The moment power spectrum

Fig. 4 –The increased percentages of internal force power spectrum with earthquake acceleration amplitudes

In order to consider the influence of different relative water depths to the hydrodynamic pressure, four conditions are calculated with the relative water depth of 0, 0.45, 0.60 and 0.75. 0.1 g is adopted for the earthquake acceleration amplitude. The shear force power spectrum and moment power spectrum at the bottom of the pier at different conditions are shown in Fig.5. As shown from the figure, the influence of the response of the pier by the hydrodynamic pressure is increasing when h_0 becomes deeper. The red circles in Fig.6 represent the increased percentage Δ at the peak value of the internal force power spectrums. Fig.6 shows that the peak values of the shear force power spectrums at the pier's bottom increase by 4%, 15% and 31% respectively, while the peak values of the moment power spectrums at the pier's bottom increase by only 1%, 4% and 9%, respectively. It shows that the hydrodynamic pressure increases the pier's repsonse under earthquake action. Moreover, the relationship between the hydrodynamic pressure and relative water depth h_0 is nonlinear and the influence of hydrodynamic pressure to the internal forces becomes more significant with the increase of relative water depth h_0.

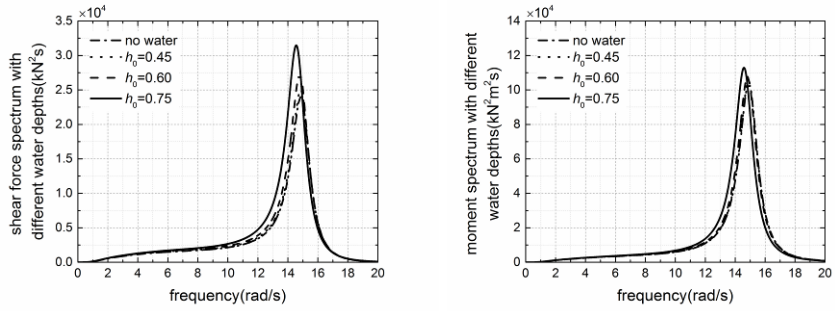

(a) The shear force power spectrum (b) The moment power spectrum

Fig. 5 –The internal force power spectrum at the pier's bottom with different relative water depths

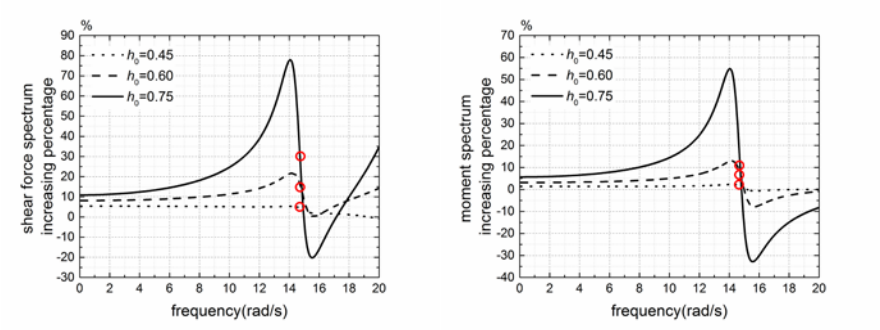

(a) The shear force power spectrum (b) The moment power spectrum

Fig. 6 –The internal force power spectrum increased percentage with different relative water depths

3.3 Stochastic dynamic analysis of the pier in deep water under wave action

Stochastic dynamic analysis of the pier in deep water under wave action is calculated, considering the wave height H_0 and relative water depth h_0 as two variables. When h_0=0.60, with H_0=2 m, 3 m and 4 m, stochastic dynamic responses of the pier are ploted in Fig.7. In addition, When H_0=2 m, with h_0=0.45, 0.60 and 0.75, the stochastic dynamic responses of the pier are shown in Fig.8.

Fig.7 shows that the internal force power spectrums increase as the wave becomes higher. However, the results shown in Fig.8 indicate that if the wave height H_0 is the same, the internal force power spectrum increase when h_0 tends to decrease. The reason is that the velocity potential decreases with the increase of h_0. Different from the responses under earthquake action, Figs.7 and 8 show that the peak values of the shear force and moment power spectrums appear at the frequency of the peak value of the wave height spectrum $S_{HH}(\omega)$.

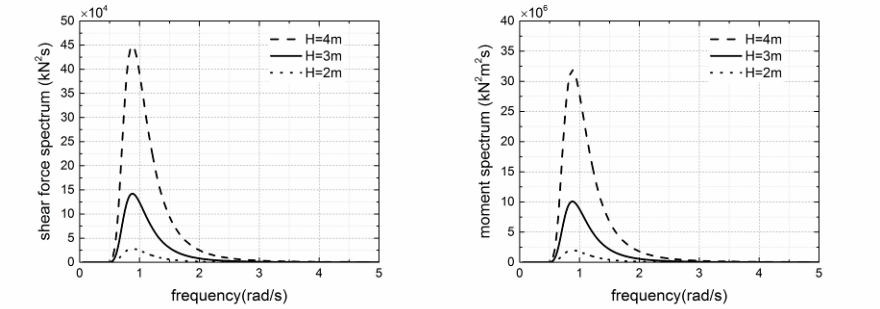

(a) The shear force power spectrum (b) The moment power spectrum

Fig. 7 –The internal force power spectrums at the pier's bottom with different wave heights

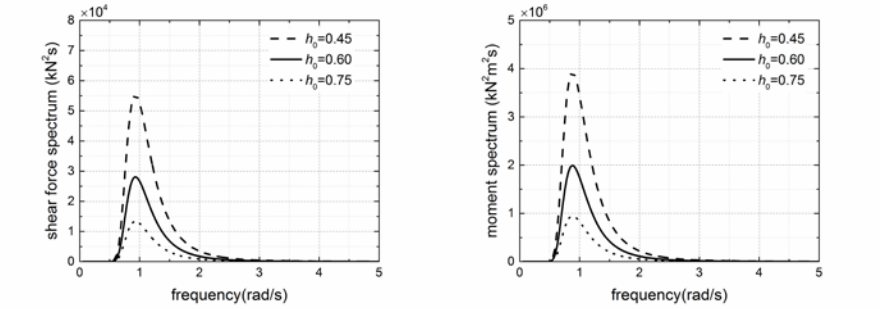

(a) The shear force power spectrum (b) The moment power spectrum

Fig. 8 –The internal force power spectrums at the pier's bottom with different water depths

3.4 Stochastic dynamic analysis of the pier in deep water under combined earthquake and wave actions

Stochastic dynamic analysis of the pier in deep water under combined earthquake and wave actions is calculated with h_0=0.60 and 0.1 g earthquake accelation amplitude. The responses of the pier under earthquake action and wave action are also added for comparision. The internal force power spectrums of two conditions are provided in Fig.9.

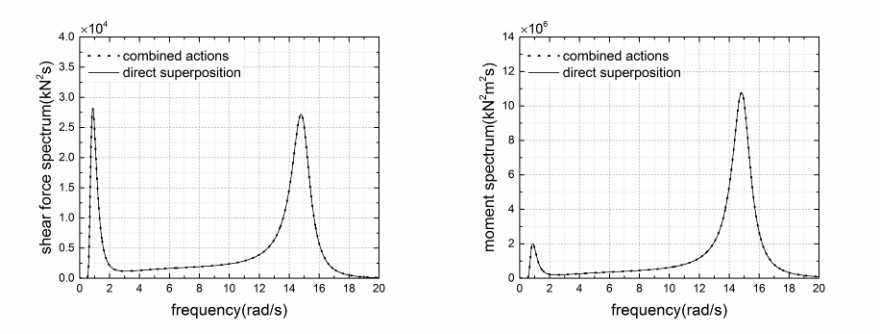

(a) The shear force power spectrum (b) The moment power spectrum

Fig. 9 –Internal force spectrums at the pier's bottom

From Fig.9, there are two peak values of the internal force power spectrums. It illustrates that the internal force power spectrums under combined earthquake and wave actions are nearly identical with these under the direct superposition of two individual actions. As it is shown in Eq. (22), the difference between combined actions and direct superpositon is that the former considers the attached mass M_2 under wave action. In this example, because the pier has high stiffness, the difference between the frequency response functions $H(\omega)$ with the mass matrix M and $M+M_2$ at every frequency is negligible. Thus, the effect of the attached mass M_2 on the frequency response function $H(\omega)$ can be ignored and the responses of two conditions are nearly identical.

4. Conclusions

(1) The stochanic dynamic response of piers in deep water is increasing because of the influence of the hydrodynamic pressure. For a pier with a fixed water depth under different earthquake acceleration amplitudes, the increased percentage of internal force power spectrums at the bottom of piers is identical, considering the effect of the hydrodynamic pressure.

(2) With relative water depth becoming deeper, the effect of the hydrodynamic pressure to the internal force power spectrums at the bottom of the pier becomes more significant. The effect of the hydrodynamic pressure under earthquake action should be considered.

(3) Because the attached mass generated by the pier's elastic motion has little effect on the frequency response function of the pier, stochanic dynamic responses under combined earthquake and wave actions are identical with these under the direct superposition of two individual actions.

5. References

[1] Nazmy AS, Abdel-Ghaffar AM. (1990). Non-linear earthquake-response analysis of long-span cable-stayed bridges: applications. *Earthquake Engineering & Structural Dynamics*, *19*(1), 63–76.

[2] Ghosn M, Chen G. (2015). Reliability of Highway Bridge Columns Under Earthquake Loading. *Lifeline Earthquake Engineering (1991)* . ASCE.

[3] Ozdemir Z, Souli M, Fahjan YM. (2010). Application of nonlinear fluid–structure interaction methods to seismic analysis of anchored and unanchored tanks. *Engineering Structures*, *32*(2), 409-423.

[4] Yeung RW. (1981). Added mass and damping of a vertical cylinder in finite-depth waters. *Applied Ocean Research*, *3*(3), 119-133.

[5] Keming S, T. N. (1991). Earthquake induced hydrodynamic pressure on axisymmetric offshore structures. *Earthquake Engineering & Structural Dynamics, 20*(5), 429–440.

[6] Lai W, Wang JJ, Shi-De HU. (2004). Earthquake induced hydrodynamic pressure on bridge pier. *Journal of Tongji University*, *32*(1), 1-5. (*in Chinese*)

[7] Walker DAG, Taylor RE. (2005). Wave diffraction from linear arrays of cylinders. *Ocean Engineering*, *32*(s 17–18), 2053-2078.

[8] Fujihashi K, Kinoshita T. (2010). Interaction of a submerged elliptic plate with waves. *Proceedings of the 9~(th) International Conference on Hydrodynamics* (Vol.22, pp.77-82).

[9] Wu BJ, Zheng YH, You YG, Jie DS, Chen Y. (2006). On diffraction and radiation problem for two cylinders in water of finite depth. *Ocean Engineering*, *33*(5), 679-704.

[10] Linton CM, Evans DV. (1990). Interaction of waves with arrays of vertical circular cylinders. *Journal of Fluid Mechanics*, *215*(-1), 549-569.

[11] Lu F, Lin JH, Kennedy D & Williams F W. (2009). An algorithm to study non-stationary random vibrations of vehicle–bridge systems.*Computers & Structures, 87*(3–4), 177-185.

[12] Fan LC., Wang JJ & Chen W. (2001). Response characteristics of long-span cable-stayed bridgesunder non-uniform seismic action.*Chinese Journal of Computational Mechanics.18*(3),358-363. (*in Chinese*)

[13] Moghaddasi M, Cubrinovski M, Chase J G, Pampanin S, & Carr A. (2011). Probabilistic evaluation of soil–foundation–structure interaction effects on seismic structural response. *Earthquake Engineering & Structural Dynamics, 40*(2), 135–154.

[14] Lin JH, Zhang W, & Li J. (1994). Structural responses to arbitrarily coherent stationary random excitations. *Computers & Structures, 50*(5), 629-633.

[15] Davenport AG. (1964). Note on the distribution of the largest value of a random function with applications to gust loading.*Proc.inst.civ.eng.paper, 28(2)*, 187-196.

[16] Vanmarcke EH, Vanmarcke EH. (1972). Properties of spectral moments with applications to random vibration. *Journal of the Engineering Mechanics Division, 98*, 425-446.